Rats and axolotls share a common molecular signature after spinal cord injury enriched in collagen-1

Athanasios Didangelos[1], Katalin Bartus[1], Jure Tica[1], Bernd Roschitzki[2], Elizabeth J. Bradbury[1]
[1]Wolfson CARD King's College London, United Kingdom. [2]Centre for functional Genomics, ETH Zurich, Switzerland.

Running title: spinal cord injury in rats and axolotls

Correspondence: A Didangelos: a.didangelos@gmail.com
Keywords: central nervous system (CNS), extracellular matrix, fibrosis, proteomics, transcriptomics, collagen, spinal cord injury

ABSTRACT

Spinal cord injury (SCI) in mammals leads to irreversible tissue damage and loss of function. In contrast, axolotls are able to fully regenerate injured tissues including the spinal cord. To explore new pathological and repair mechanisms, we compared rat versus axolotl transcriptomics microarrays and isolated shared genes that were similarly or differentially regulated between the two species 7 days post-SCI. Functionally distinct groups of genes characterised rat and axolotl transcriptional profiles after spinal injury. Unexpectedly, multiple genes involved in extracellular matrix remodelling, and in particular collagen-1 (type I collagen; COL1A) and collagen-associated molecules, were upregulated in both rats and axolotls after SCI. Given the significance of collagen-1 and matrix remodelling in scarring and fibrosis in mammals, we examined collagen-1 further in rat contusion SCI. High-throughput proteomics analysis validated the persistent and robust expression of the collagen-enriched matrix signature at the protein level. Collagen-1 accumulated abundantly both in early and advanced rat contusion lesions. Surprisingly, collagen-1 accumulation was likely not due to tissue fibrosis but was instead associated with pathological vascular remodelling. The transcription factor SP1 which was upregulated after SCI, was database predicted and further validated to regulate, at least in part, the expression of collagen-1 and associated proteins in rat lesions. Our work reveals the unexpected contribution of collagen-1 and vascular remodelling to scarring in rat contusion SCI. Regulation of collagen and vascular remodelling might represent novel therapeutic targets for blocking or reversing tissue scarring after mammalian SCI.

Severe injuries to the mammalian spinal cord are characterised by lack of positive wound healing and regeneration and often result in permanent functional impairment (1). Following SCI, chronic inflammation and reactive gliosis drive neuronal loss and irreversible tissue scarring (2,3). The maladaptive inflammatory response and accumulation of extracellular matrix (ECM) proteins in lesions, especially large chondroitin-sulfate proteoglycans (4,5), are the major pathological determinants and are largely responsible for the lack of neuronal regeneration after SCI (6,7). Although significant advancements have been made in understanding pathological as well as regenerative mechanisms in SCI, there are no therapies that can promote complete tissue repair.

In contrast to mammals, amphibian urodela such as axolotl mexicanum have the ability to fully regenerate most tissues including the spinal cord (8,9). While the mechanisms behind this remarkable ability are not entirely understood, previous work points towards the combined molecular effect of progenitors, excellent patterning and a very effective immune response (10-12). Mammalian SCI has not been compared extensively to axolotls, yet such comparisons have the potential to identify conserved molecular mechanisms with unknown pathological or regenerative potential in SCI (13).

METHODS

Rat and Axolotl microarray data: Rat T7 spinal clip compression injury (7 days) microarray (14) was obtained from GEO-NCBI (**goo.gl/Hz4Gj9**). Axolotl mexicanum spinal cord injury

microarray (9) data was obtained from the same server (**goo.gl/Eoshgn**). More details in **Supplemental Methods.**

SCI model: Isofluorane anesthetized female adult Sprague-Dawley rats (~200g; Harlan Laboratories, UK) received a midline 150 kdyne contusion injury at spinal level T10 using an Infinite Horizon impactor device, as previously described in (15). Control T10 spinal cord tissue was collected from uninjured animals of the same sex, strain and weight. The study has received approval by King's College London under licence and all surgical procedures were performed in accordance with the United Kingdom Animals (Surgical Procedures) Act 1996. More information in **Supplemental Methods**.

Protein extraction from spinal cords and shot-gun proteomics: Protein extraction from either T10 injury epicentre or uninjured control T10 spinal cord segments (5–6 mm, ~45 mg per explant covering the entire injury epicentre) was performed on PBS-EDTA perfused rats using a protein extraction protocol to ensure sequential isolation of cellular (0.08% SDS) and extracellular (4M guanidine) proteins from spinal cords. Liquid chromatography tandem mass-spectrometry shot-gun proteomics (Q Exactive hybrid quadrupole orbitrap) was performed on both 0.08% SDS and 4M guanidine spinal cord tissue extracts from 3 intact and 3 injured (7 days post-SCI) T10 spinal cord segments as previously published in considerable detail (16). Raw MS/MS data was loaded for protein, peptide and spectra validation and visualization onto Scaffold v4 (17). Scaffold was also used to calculate normalised spectral counts for quantitation (18). Protein extraction and proteomics procedures are described in-depth in **Supplemental Methods**.

Immunoblotting: Protein extracts were electrophoresed and immunoblotted using standard and routine protocols (5,16). 16µg of protein per sample were separated on 15-well, 4–12% pre-cast gradient gels (NuPAGE, Invitrogen). Proteins were transferred on nitrocellulose membranes, blocked and incubated with 1ry antibodies (1:1000) for 16h at 4^0C. Membranes were washed and incubated with appropriate horseradish peroxidase-conjugated 2ry antibodies (1:2000; Dako). Finally, enhanced chemiluminescence (ECL) signals were visualised in a UVP BioSpectrum. More information and antibodies used in **Supplemental Methods**.

Quantitative PCR: Total RNA was extracted from intact and injured T10 spinal cord tissue explants homogenised in Trizol reagent (Sigma) and using routine protocols (5,16). RNA was purified using the EZNA total RNA kit I (Omega Bio-Tek). 2000 ng of RNA per sample were converted into cDNA using an RNA-to-cDNA kit (Applied Biosystems). 20 ng of RNA per reaction were quantified using rat prevalidated TaqMan primer/probe mixes for CD34, PDGFR, COLA1 and COL1A2 (Applied Biosystems). GAPDH was the housekeeper. Real-time PCR was performed using a Roche thermocycler. Fold-change in mRNA expression of target genes was calculated relative to intact T10 explants using the ΔΔCt method. More details in **Supplemental Methods**.

Immunohistochemistry: T10 SCI epicentre or intact T10 spinal cord segments were collected from 4% PFA perfused-fixed animals (60min total fixation time). 30µm cryosections were probed with goat CD34 (1:100; RnD), rabbit COL1A1/A2 (1:100; Abcam), rabbit PDGFRα antibodies (1:100; Cell Signalling) and rabbit CD45 (1:100; Abcam). Sections were incubated for 16 h at 4°C and received either donkey anti-rabbit AlexaFluor 568 or donkey anti-goat AlexaFluor 488 for 90 min. Sections were mounted using VectaStain and imaged on a Zeiss Axioplan 2 microscope. More details in **Supplemental Methods**.

Statistical and Computational analysis: Differential protein expression was measured using spectral counting (Scaffold v4). Differential protein levels were estimated by unpaired, two-tailed T-Test for each identified protein. No outliers were removed. Hierarchical clustering and heat-maps were made in TM4 MeV v4.8 (19). Protein-protein interaction networks were

created using StringDB v10 (20). Protein networks were visualised in CytoScape v2.8 (21) and analysed using BinGO (22) to identify overrepresented Biological Process GO terms. Densitometry and TaqMan qPCR data were analysed using T-Test. GraphPad Prism v6 was used to carry out all statistical tests and obtain *p* values. Additional details in **Supplemental Methods**.

RESULTS

Rat and axolotl transcriptomics microarrays comparison: To identify molecular differences and similarities between rats and axolotls we performed an intersection of differentially regulated genes identified in a rat SCI microarray (14) 7 days after injury (**Supplemental table 1**) with differentially regulated genes identified in a microarray dataset of axolotl mexicanum SCI (9) also 7 days post-injury (**Supplemental table 2**). Both datasets are freely accessible via the gene expression omnibus (GEO-NCBI; Rat: goo.gl/Hz4Gj9 and Axolotl: goo.gl/Eoshgn). Microarray data from GEO is qualitatively and statistically curated and MIAME-compliant (23). Significantly upregulated and downregulated genes from rat and axolotl microarrays are also visualised and qualitatively analysed as protein-protein interaction networks in **Supplemental Fig. 1** and **Supplemental Fig. 2** respectively.

Next, we compared the datasets to find transcripts that were shared and significantly altered in both species at 7 days post-SCI. Only genes that had adjusted *p* value of ≤0.05 and fold-change ≥2 were included (**Supplemental Tables 1 & 2**). We found 4 groups of shared genes (**Fig. 1A**): *Group 1* with 153 genes upregulated in axolotls but downregulated in rats; *Group 2* with 156 genes that were upregulated in both axolotls and rats; *Group 3* with 77 genes downregulated in both axolotls and rats; *Group 4* with 228 genes downregulated in axolotls but upregulated in rats. While rats and axolotls share 156 upregulated genes (**Fig. 1B**; 50.4% similarity), only 77 genes are downregulated in both species, while 228 of the genes that are downregulated in axolots are instead overexpressed in rats (**Fig. 1B**; 25.2% similarity). We then used BinGO (22) to identify overrepresented biological process gene ontology (GO) terms in each group of shared genes. Genes present in each group together with overrepresented GO terms are presented in **Supplemental Fig. 3**. *Group 1* was characterised by "neuronal development" and "neuron projection" terms (**Fig. 1A** & **Supplemental Fig. 3A**) perhaps reflecting that multiple neuronal transcripts are downregulated in rats but instead are increased in regenerating axolotls after SCI. *Group 2* (upregulated in both species) was enriched in "extracellular matrix organization" (**Fig. 1A** & **Supplemental Fig. 3B**) indicating that matrix remodelling is involved in wound healing in both species. This complex group contained multiple collagen genes (including collagen-1; COL1A1 & COL1A2), but also "response to wounding" (mainly inflammatory genes), "cell adhesion/motility" and "vascular development" terms (**Supplemental Fig. 3B**). *Group 3* (genes reduced in both species) was characterised by "sterol/lipid metabolism" terms (**Fig. 1A** & **Supplemental Fig. 3C**). Cholesterol synthesis is reduced during peripheral nerve regeneration (24). *Group 4* was enriched in "nucleic acid metabolism" and "cell cycle" terms (**Fig. 1A** & **Supplemental Fig. 3D**), perhaps unsurprisingly given the importance of cell cycle regulation in axolotls regeneration (25).

The upregulation of extracellular matrix entities in both rats and axolotls after SCI (*Group 2*), in particular collagen-1 (COL1A1 and COL1A2), other collagens (COL3A1, COL4A1/A2, COL5A1/A2 and COL12A1), matrix and collagen-associated molecules (LUM, FN1, TNC, PXDN, POSTN, SERPINH1 and MMP2; genes highlighted in **Fig. 1C**), was interesting given that matrix accumulation is characteristic of fibrosis, the cardinal feature of tissue pathology and degeneration in most mammalian organs (26). Importantly, the central nervous system is generally considered to be devoid of classic fibrosis and collagen-1, especially in injuries that do not penetrate the meninges (27,28).

Proteomics validates the upregulation of the collagen-1 signature in rats: To identify molecules that showed consistent differential regulation after mammalian SCI at the mRNA and protein level, we performed spinal cord proteomics in rats comparing intact T10 spinal cord segments with T10 injury epicentres 7 days post-SCI, using shot-gun proteomics and

label-free protein quantitation with spectral counting (18,29). To achieve high-sensitivity, we used tissue processing previously developed in our lab which allows the sequential extraction and analysis of mainly cellular proteins (detergent-soluble) in 0.08% SDS, followed by the extraction of highly cross-linked extracellular matrix proteins (detergent-insoluble) in 4M guanidine (16,29,30). All protein identifications and spectral counts from SDS and guanidine extracts are shown in **Supplemental Table 3** and **Supplemental Table 4** respectively. All raw LC-MS/MS and processed data is publically available in *Mendeley Data for Journals* (SDS: goo.gl/3xjtjq & goo.gl/s8L6La; Guanidine: goo.gl/6zE2fP & goo.gl/8ZtEUH). We then compared the proteomics data with the rat microarray. The SDS proteomics dataset (**Supplemental Table 3**) was used for the intersection of all identified tissue proteins excluding extracellular proteins, which were retrieved from the guanidine dataset (extracellular proteins are indicated in **Supplemental Table 4**). Comparison of rat transcriptomics and proteomics returned 110 molecules that were upregulated and 90 molecules that were downregulated both at the mRNA and protein level 7 days after rat SCI, summarised in **Supplemental Fig. 4**.

When these signatures were compared to the axolotl transcriptomics dataset we found 35 common molecules upregulated in axolotls (**Fig. 2A, C**) and 26 common molecules downregulated in axolotls (**Fig. 2B, D**). Heat-maps (**Fig. 2A-B**) display differential expression from proteomics of rat SCI. Again, shared upregulated molecules included multiple collagens and collagen-associated proteins (**Fig. 2C**), confirming the transcriptomics findings (see *Group 2* **Fig. 1A, C**). Interestingly, many of these matrix proteins were recently found by our group using proteomics in advanced (8 week) T10 rat lesions (16). This consistent signature suggests a conserved response in both species that is related to collagen and potentially vascular remodelling and might be associated with regeneration in the axolotl but tissue scarring in the rat. The cluster of common molecules downregulated in the axolotl was associated with "sterol/lipid biosynthesis" (**Fig. 2D**), again confirming the transcriptomics comparison (see *Group 3;* **Fig. 1A**).

Multiple upregulated proteins from the signature were then validated by western-blotting in lesions from a separate cohort of rats 7 days post-injury (**Fig. 2E**). These included classic SCI proteins fibronectin (FN1), IBA1 (macrophage/microglia marker) and vimentin (VIM; astrocytes, fibroblasts and endothelial cells). Other less known proteins included the collagen-associated proteoglycan lumican (LUM) as well as SERPINH1 (Hsp47) and peptidase D (PEPD), both involved in collagen-1 metabolism. Beta 3 Tubulin (TUBB3), a typical neuronal marker, was clearly downregulated after rat SCI as expected (31), but was instead upregulated in axolotls 7 days after SCI (**Fig. 2A**), indicating the difference in neuronal regeneration between the two species.

Accumulation of collagen-1 in rat lesions: Collagen-1 was examined further in a separate cohort of SCI rats. Immunohistological localization in spinal lesions found a clear upregulation and accumulation of COL1A (antibody recognises both COL1A1 and COL1A2 chains) after SCI (**Fig. 3A-B**) in comparison to intact T10 sections (**Fig. 3D-E**). Collagen was apparent as a dense meshwork within the lesion core and colocalized with CD34 (**Fig. 3B**), a surface marker highly abundant in endothelial cells and endothelial progenitors, enriched in capillaries, microvessels and small proliferating vessels during angiogenesis (32-37). Costained areas showed a disorganised microvessel appearance indicative of abberant vascular remodelling (**Fig. 3B**). CD34 also stained individual globular cells around collagen-stained areas, presumably lesion-infiltrating endothelial progenitors (**Fig. 3A-B**). High-magnification revealed contact between CD34+ cells with collagen-stained microvessels as well as clear endothelial staining (**Fig. 3C**; white arrows). Intact T10 spinal cord sections (**Fig. 3D-E**) had extensive CD34 staining in grey matter capillaries (**Fig. 3E**; *cp*), while COL1A stained larger vessels in white and grey matter (**Fig. 3E**; *vs*).

In consecutive serial sections (30μm apart) the lesion core, where most of collagen-1 staining was seen (**Fig. 3A-B**), was also immunopositive for PDGFRα (**Fig. 3F-G**), suggesting that collagen might be expressed by perivascular cells from injured vessels, as shown before in mouse SCI, with pericytes and perivascular fibroblasts suggested as the main

collagen sources (38,39). CD34+ cells were associated with PDGFRα+ regions but they did not apper to colocalize (**Fig. 3F-H**). Upregulation of COL1A1, COL1A2, CD34 and PDGFRα was validated at the mRNA level, in a separate cohort of injured animals (**Fig. 3K**). In advanced cavitated lesions (12 weeks post-SCI), collagen-1 staining was extensive (**Supplemental Fig. 5A-B**). Similar to 2 weeks post-injury (**Fig. 3A-B**), COL1A and CD34 colocalised and the staining pattern was consistent with erratic microvessels (**Supplemental Fig. 5B**).

SP1 regulates collagen-1 in rat lesions: Transcription factor promoter binding site analysis (MSigDB-TRANSFAC; 40,41) found that SP1 was the potential regulator of the highest number of collagen-signature genes (16 genes with likely SP1 promoter binding sites; **Fig. 3L**). SP1 was also increased at the protein level following rat SCI (**Fig. 2E**), and in agreement with rat microarray data (**Supplemental Fig. 1H**). In proof-of-concept experiments, the potential involvement of SP1 in collagen regulation was tested using mithramycin (**Fig. 3M-N**), a drug that binds to DNA sequences with guanosine–cytosine (GC) base specificity and interferes with GC-binding transcription factors, such as SP1 (42). Intraperitoneal injections of mithramycin for 14 days following rat SCI (0.2mg/kg; 43,44) reduced the expression of collagen-signature proteins with predicted SP1 DNA-binding sites including COL1A1 and COL1A2, PEPD, VIM and SP1 itself (**Fig. 3M-N**). Mithramycin injections also reduced the prime angiogenic protein, vascular endothelial growth factor A (VEGFA; **Fig. 3M-N**), also known to be regulated by SP1 (45). Fibronectin (FN1) was only marginally affected. Thus, SP1 might regulate matrix remodelling genes after SCI. Nevertheless, we cannot rule out the possibility that other GC-binding transcription factors might also be affected by mithramycin (notably SP3; 46) and may play a role in regulating this gene signature.

DISCUSSION

Here we performed for the first time a multi-parametric comparison of rat and axolotl spinal cord injury using high-throughput transcriptomics and proteomics. This approach is unique as it directly examined gene expression differences and similarities between a clinically relevant model of mammalian SCI in rats, with a highly regenerative model of SCI in axolotls. The primary comparative analysis as well as the independently validated findings reported here, were based on recently published studies and publically available microarray and proteomics datasets, highlighting the importance of sharing high-throughput data. Amongst multiple interesting findings, the transcriptomics comparison revealed an extracellular matrix collagen-enriched gene cluster that was upregulated in both rats and axolotls after SCI and was subsequently validated using high-throughput proteomics in rats. While expression of collagen-1 has been shown in murine SCI (38,39), little is known about collagen and fibrosis in clinically relevant rat contusion SCI (28,47).

In rats, the unexpected accumulation of collagen-1 in the injury site started early and persisted chronically. Rather than loose interstitial fibrosis that typically affects injured mammalian organs, it appears that collagen-1 accumulation was related to aberrant vascular remodelling as collagen-1 colocalised with an abundance of CD34+ cells and disorganised CD34-stained microvessels. CD34+ cells likely represent a population of existing endothelial cells or progenitors that proliferate out of surviving capillaries (CD34 is abundant in grey matter capillaries -34) in the injury epicentre and penumbra, and participate together with collagen-1 to vascular remodelling (32,48,49). CD34+ cells might also be infiltrating (50,51) hematopoietic or myeloid progenitors (52) but this is less likely as we found that they are distinct from abundant CD45+ cells (leukocytes and macrophages/microglia) in spinal lesions (**Supplemental Fig. 6**). The origin of collagen-1 in rat lesions is unknown but it might be expressed by PDGFR+ perivascular fibroblasts or pericytes as previously shown in mice (38,39). Phenotypically complex vascular pericytes are recently gaining attention as major players of collagen expression and fibrosis in different mammalian organs (53,54).

In both rats and axolotls collagen and vascular remodelling after SCI might be linked and likely represent a conserved mechanism aimed at wound healing and regeneration, given that blood vessels provide trophic support to injured tissues. Although vascular remodelling is

evidently incomplete and fails to support tissue repair in rats, it is presumably highly effective and organised in axolotls and might represent an important factor in their regenerative process (11). Surprisingly, the role and mechanisms of angiogenesis in axolotls have not been studied in detail, even with regards to limb regeneration (55), and represent interesting areas for future investigations. In mammalian SCI, the role of angiogenesis has been debated, with protective, neutral or even detrimental effects proposed, and more work is required to clarify (50,56-59). Perhaps future repair-promoting strategies should focus not in enhancing angiogenesis but instead in limiting excess collagen-1 deposition (grey matter capillaries are acollagenous) and potentially in organising vessel formation. For instance, organised vascular remodelling was recently shown to be critical for anatomical and functional regeneration in the peripheral nervous system, which regenerates rather effectively. New blood vessels forming in peripheral nerves after injury act as tracks onto which myelinating cells (Schwann cells) are spatially orientated during neuronal regeneration (60).

Another interesting finding was the upregulation of SP1 after rat SCI. The ubiquitous transcription factor was predicted to regulate many genes in the collagen signature and in proof-of-concept experiments, the non-selective SP1 inhibitor mithramycin reduced the expression of collagen-1, VEGFA and others. While these findings are perhaps unsurprising given the role of SP1 in the regulation of thousands of genes including collagen-1, fibrosis and angiogenesis transcripts (45,61,62), it is worth noting that its potential function after SCI has not been studied at all to this date.

In summary, comparison of rat and axolotl SCI transcriptomics revealed that genes involved in matrix remodelling were upregulated in both species. Not only was the excessive accumulation of collagen-1 following rat spinal contusion unexpected but in addition, the potential association of collagen with pathological vascular remodelling is described here for the first time. Collagen accumulation and vascular remodelling are interesting targets for future therapeutic approaches to mammalian SCI. Finally, our publically-available comparative high-throughput analysis identified a multitude of new genes that were similarly or differentially regulated between the two species and could form the basis for future studies in our field an beyond.

REFERENCES

1. Ramer, L. M., Ramer, M. S., and Bradbury, E. J. (2014) Restoring function after spinal cord injury: towards clinical translation of experimental strategies *Lancet Neurol* **13**, 1241-1256
2. Fitch, M. T., and Silver, J. (2008) CNS injury, glial scars, and inflammation: Inhibitory extracellular matrices and regeneration failure *Exp Neurol* **209**, 294-301
3. Gaudet, A. D., and Popovich, P. G. (2014) Extracellular matrix regulation of inflammation in the healthy and injured spinal cord *Exp Neurol* **258**, 24-34
4. Bradbury, E. J., Moon, L. D., Popat, R. J., King, V. R., Bennett, G. S., Patel, P. N., Fawcett, J. W., and McMahon, S. B. (2002) Chondroitinase ABC promotes functional recovery after spinal cord injury *Nature* **416**, 636-640
5. Didangelos, A., Iberl, M., Vinsland, E., Bartus, K., and Bradbury, E. J. (2014) Regulation of IL-10 by chondroitinase ABC promotes a distinct immune response following spinal cord injury *J Neurosci* **34**, 16424-16432
6. Benowitz, L. I., and Popovich, P. G. (2011) Inflammation and axon regeneration *Curr Opin Neurol* **24**, 577-583
7. David, S., and Kroner, A. (2011) Repertoire of microglial and macrophage responses after spinal cord injury *Nat Rev Neurosci* **12**, 388-399
8. Rodrigo Albors, A., Tazaki, A., Rost, F., Nowoshilow, S., Chara, O., and Tanaka, E. M. (2015) Planar cell polarity-mediated induction of neural stem cell expansion during axolotl spinal cord regeneration *Elife* **4**, e10230
9. Sabin, K., Santos-Ferreira, T., Essig, J., Rudasill, S., and Echeverri, K. (2015) Dynamic membrane depolarization is an early regulator of ependymoglial cell response to spinal cord injury in axolotl *Dev Biol* **408**, 14-25

10. Echeverri, K., and Tanaka, E. M. (2002) Ectoderm to mesoderm lineage switching during axolotl tail regeneration *Science* **298**, 1993-1996
11. Godwin, J. W., Pinto, A. R., and Rosenthal, N. A. (2013) Macrophages are required for adult salamander limb regeneration *Proc Natl Acad Sci U S A* **110**, 9415-9420
12. Tanaka, E. M. (2016) The Molecular and Cellular Choreography of Appendage Regeneration *Cell* **165**, 1598-1608
13. Diaz Quiroz, J. F., Tsai, E., Coyle, M., Sehm, T., and Echeverri, K. (2014) Precise control of miR-125b levels is required to create a regeneration-permissive environment after spinal cord injury: a cross-species comparison between salamander and rat *Dis Model Mech* **7**, 601-611
14. Chamankhah, M., Eftekharpour, E., Karimi-Abdolrezaee, S., Boutros, P. C., San-Marina, S., and Fehlings, M. G. (2013) Genome-wide gene expression profiling of stress response in a spinal cord clip compression injury model *BMC Genomics* **14**, 583
15. James, N. D., Bartus, K., Grist, J., Bennett, D. L., McMahon, S. B., and Bradbury, E. J. (2011) Conduction failure following spinal cord injury: functional and anatomical changes from acute to chronic stages *J Neurosci* **31**, 18543-18555
16. Didangelos, A., Puglia, M., Iberl, M., Sanchez-Bellot, C., Roschitzki, B., and Bradbury, E. J. (2016) High-throughput proteomics reveal alarmins as amplifiers of tissue pathology and inflammation after spinal cord injury *Sci Rep* **6**, 21607
17. Searle, B. C. (2010) Scaffold: a bioinformatic tool for validating MS/MS-based proteomic studies *Proteomics* **10**, 1265-1269
18. Arike, L., and Peil, L. (2014) Spectral counting label-free proteomics *Methods Mol Biol* **1156**, 213-222
19. Saeed, A. I., Bhagabati, N. K., Braisted, J. C., Liang, W., Sharov, V., Howe, E. A., Li, J., Thiagarajan, M., White, J. A., and Quackenbush, J. (2006) TM4 microarray software suite *Methods Enzymol* **411**, 134-193
20. Szklarczyk, D., Franceschini, A., Wyder, S., Forslund, K., Heller, D., Huerta-Cepas, J., Simonovic, M., Roth, A., Santos, A., Tsafou, K. P., Kuhn, M., Bork, P., Jensen, L. J., and von Mering, C. (2015) STRING v10: protein-protein interaction networks, integrated over the tree of life *Nucleic Acids Res* **43**, D447-452
21. Smoot, M. E., Ono, K., Ruscheinski, J., Wang, P. L., and Ideker, T. (2010) Cytoscape 2.8: new features for data integration and network visualization *Bioinformatics* **27**, 431-432
22. Maere, S., Heymans, K., and Kuiper, M. (2005) BiNGO: a Cytoscape plugin to assess overrepresentation of gene ontology categories in biological networks *Bioinformatics* **21**, 3448-3449
23. Barrett, T., Suzek, T. O., Troup, D. B., Wilhite, S. E., Ngau, W. C., Ledoux, P., Rudnev, D., Lash, A. E., Fujibuchi, W., and Edgar, R. (2005) NCBI GEO: mining millions of expression profiles--database and tools *Nucleic Acids Res* **33**, D562-566
24. Goodrum, J. F. (1990) Cholesterol synthesis is down-regulated during regeneration of peripheral nerve *J Neurochem* **54**, 1709-1715
25. Heber-Katz, E., Zhang, Y., Bedelbaeva, K., Song, F., Chen, X., and Stocum, D. L. (2012) Cell cycle regulation and regeneration *Curr Top Microbiol Immunol* **367**, 253-276
26. Wynn, T. A. (2007) Common and unique mechanisms regulate fibrosis in various fibroproliferative diseases *J Clin Invest* **117**, 524-529
27. Klapka, N., and Muller, H. W. (2006) Collagen matrix in spinal cord injury *J Neurotrauma* **23**, 422-435
28. Moeendarbary, E., Weber, I. P., Sheridan, G. K., Koser, D. E., Soleman, S., Haenzi, B., Bradbury, E. J., Fawcett, J., and Franze, K. (2017) The soft mechanical signature of glial scars in the central nervous system *Nat Commun* **8**, 14787
29. Didangelos, A., Yin, X., Mandal, K., Baumert, M., Jahangiri, M., and Mayr, M. (2010) Proteomics characterization of extracellular space components in the human aorta *Mol Cell Proteomics* **9**, 2048-2062

30. Didangelos, A., Yin, X., Mandal, K., Saje, A., Smith, A., Xu, Q., Jahangiri, M., and Mayr, M. (2011) Extracellular matrix composition and remodeling in human abdominal aortic aneurysms: a proteomics approach *Mol Cell Proteomics* **10**, M111 008128
31. Hellal, F., Hurtado, A., Ruschel, J., Flynn, K. C., Laskowski, C. J., Umlauf, M., Kapitein, L. C., Strikis, D., Lemmon, V., Bixby, J., Hoogenraad, C. C., and Bradke, F. (2011) Microtubule stabilization reduces scarring and causes axon regeneration after spinal cord injury *Science* **331**, 928-931
32. Chao, H., and Hirschi, K. K. (2010) Hemato-vascular origins of endothelial progenitor cells? *Microvasc Res* **79**, 169-173
33. Goon, P. K., Lip, G. Y., Boos, C. J., Stonelake, P. S., and Blann, A. D. (2006) Circulating endothelial cells, endothelial progenitor cells, and endothelial microparticles in cancer *Neoplasia* **8**, 79-88
34. Kalaria, R. N., and Kroon, S. N. (1992) Expression of leukocyte antigen CD34 by brain capillaries in Alzheimer's disease and neurologically normal subjects *Acta Neuropathol* **84**, 606-612
35. Ohmori, S., Shiraki, K., Sugimoto, K., Sakai, T., Fujikawa, K., Wagayama, H., Takase, K., and Nakano, T. (2001) High expression of CD34-positive sinusoidal endothelial cells is a risk factor for hepatocellular carcinoma in patients with HCV-associated chronic liver diseases *Hum Pathol* **32**, 1363-1370
36. Pusztaszeri, M. P., Seelentag, W., and Bosman, F. T. (2006) Immunohistochemical expression of endothelial markers CD31, CD34, von Willebrand factor, and Fli-1 in normal human tissues *J Histochem Cytochem* **54**, 385-395
37. Siemerink, M. J., Klaassen, I., Vogels, I. M., Griffioen, A. W., Van Noorden, C. J., and Schlingemann, R. O. (2012) CD34 marks angiogenic tip cells in human vascular endothelial cell cultures *Angiogenesis* **15**, 151-163
38. Goritz, C., Dias, D. O., Tomilin, N., Barbacid, M., Shupliakov, O., and Frisen, J. (2011) A pericyte origin of spinal cord scar tissue *Science* **333**, 238-242
39. Soderblom, C., Luo, X., Blumenthal, E., Bray, E., Lyapichev, K., Ramos, J., Krishnan, V., Lai-Hsu, C., Park, K. K., Tsoulfas, P., and Lee, J. K. (2013) Perivascular fibroblasts form the fibrotic scar after contusive spinal cord injury *J Neurosci* **33**, 13882-13887
40. Liberzon, A., Birger, C., Thorvaldsdottir, H., Ghandi, M., Mesirov, J. P., and Tamayo, P. (2016) The Molecular Signatures Database (MSigDB) hallmark gene set collection *Cell Syst* **1**, 417-425
41. Matys, V., Fricke, E., Geffers, R., Gossling, E., Haubrock, M., Hehl, R., Hornischer, K., Karas, D., Kel, A. E., Kel-Margoulis, O. V., Kloos, D. U., Land, S., Lewicki-Potapov, B., Michael, H., Munch, R., Reuter, I., Rotert, S., Saxel, H., Scheer, M., Thiele, S., and Wingender, E. (2003) TRANSFAC: transcriptional regulation, from patterns to profiles *Nucleic Acids Res* **31**, 374-378
42. Yuan, P., Wang, L., Wei, D., Zhang, J., Jia, Z., Li, Q., Le, X., Wang, H., Yao, J., and Xie, K. (2007) Therapeutic inhibition of Sp1 expression in growing tumors by mithramycin a correlates directly with potent antiangiogenic effects on human pancreatic cancer *Cancer* **110**, 2682-2690
43. Chatterjee, S., Zaman, K., Ryu, H., Conforto, A., and Ratan, R. R. (2001) Sequence-selective DNA binding drugs mithramycin A and chromomycin A3 are potent inhibitors of neuronal apoptosis induced by oxidative stress and DNA damage in cortical neurons *Ann Neurol* **49**, 345-354
44. Ferrante, R. J., Ryu, H., Kubilus, J. K., D'Mello, S., Sugars, K. L., Lee, J., Lu, P., Smith, K., Browne, S., Beal, M. F., Kristal, B. S., Stavrovskaya, I. G., Hewett, S., Rubinsztein, D. C., Langley, B., and Ratan, R. R. (2004) Chemotherapy for the brain: the antitumor antibiotic mithramycin prolongs survival in a mouse model of Huntington's disease *J Neurosci* **24**, 10335-10342
45. Pore, N., Liu, S., Shu, H. K., Li, B., Haas-Kogan, D., Stokoe, D., Milanini-Mongiat, J., Pages, G., O'Rourke, D. M., Bernhard, E., and Maity, A. (2004) Sp1 is involved in

Akt-mediated induction of VEGF expression through an HIF-1-independent mechanism *Mol Biol Cell* **15**, 4841-4853
46. Li, L., He, S., Sun, J. M., and Davie, J. R. (2004) Gene regulation by Sp1 and Sp3 *Biochem Cell Biol* **82**, 460-471
47. Cregg, J. M., DePaul, M. A., Filous, A. R., Lang, B. T., Tran, A., and Silver, J. (2014) Functional regeneration beyond the glial scar *Exp Neurol* **253**, 197-207
48. Patel, J., Seppanen, E. J., Rodero, M. P., Wong, H. Y., Donovan, P., Neufeld, Z., Fisk, N. M., Francois, M., and Khosrotehrani, K. (2017) Functional Definition of Progenitors Versus Mature Endothelial Cells Reveals Key SoxF-Dependent Differentiation Process *Circulation* **135**, 786-805
49. Rookmaaker, M. B., Verhaar, M. C., Loomans, C. J., Verloop, R., Peters, E., Westerweel, P. E., Murohara, T., Staal, F. J., van Zonneveld, A. J., Koolwijk, P., Rabelink, T. J., and van Hinsbergh, V. W. (2005) CD34+ cells home, proliferate, and participate in capillary formation, and in combination with CD34- cells enhance tube formation in a 3-dimensional matrix *Arterioscler Thromb Vasc Biol* **25**, 1843-1850
50. Graumann, U., Ritz, M. F., and Hausmann, O. (2011) Necessity for re-vascularization after spinal cord injury and the search for potential therapeutic options *Curr Neurovasc Res* **8**, 334-341
51. Hausmann, O. N. (2003) Post-traumatic inflammation following spinal cord injury *Spinal Cord* **41**, 369-378
52. Asahara, T., Murohara, T., Sullivan, A., Silver, M., van der Zee, R., Li, T., Witzenbichler, B., Schatteman, G., and Isner, J. M. (1997) Isolation of putative progenitor endothelial cells for angiogenesis *Science* **275**, 964-967
53. Birbrair, A., Zhang, T., Files, D. C., Mannava, S., Smith, T., Wang, Z. M., Messi, M. L., Mintz, A., and Delbono, O. (2014) Type-1 pericytes accumulate after tissue injury and produce collagen in an organ-dependent manner *Stem Cell Res Ther* **5**, 122
54. Leaf, I. A., Nakagawa, S., Johnson, B. G., Cha, J. J., Mittelsteadt, K., Guckian, K. M., Gomez, I. G., Altemeier, W. A., and Duffield, J. S. (2017) Pericyte MyD88 and IRAK4 control inflammatory and fibrotic responses to tissue injury *J Clin Invest* **127**, 321-334
55. Smith, A. R., and Wolpert, L. (1975) Nerves and angiogenesis in amphibian limb regeneration *Nature* **257**, 224-225
56. Benton, R. L., Maddie, M. A., Gruenthal, M. J., Hagg, T., and Whittemore, S. R. (2009) Neutralizing endogenous VEGF following traumatic spinal cord injury modulates microvascular plasticity but not tissue sparing or functional recovery *Curr Neurovasc Res* **6**, 124-131
57. Benton, R. L., and Whittemore, S. R. (2003) VEGF165 therapy exacerbates secondary damage following spinal cord injury *Neurochem Res* **28**, 1693-1703
58. Kao, C. H., Chen, S. H., Chio, C. C., and Lin, M. T. (2008) Human umbilical cord blood-derived CD34+ cells may attenuate spinal cord injury by stimulating vascular endothelial and neurotrophic factors *Shock* **29**, 49-55
59. Widenfalk, J., Lipson, A., Jubran, M., Hofstetter, C., Ebendal, T., Cao, Y., and Olson, L. (2003) Vascular endothelial growth factor improves functional outcome and decreases secondary degeneration in experimental spinal cord contusion injury *Neuroscience* **120**, 951-960
60. Cattin, A. L., Burden, J. J., Van Emmenis, L., Mackenzie, F. E., Hoving, J. J., Garcia Calavia, N., Guo, Y., McLaughlin, M., Rosenberg, L. H., Quereda, V., Jamecna, D., Napoli, I., Parrinello, S., Enver, T., Ruhrberg, C., and Lloyd, A. C. (2015) Macrophage-Induced Blood Vessels Guide Schwann Cell-Mediated Regeneration of Peripheral Nerves *Cell* **162**, 1127-1139
61. Tan, N. Y., and Khachigian, L. M. (2009) Sp1 phosphorylation and its regulation of gene transcription *Mol Cell Biol* **29**, 2483-2488
62. Verrecchia, F., Rossert, J., and Mauviel, A. (2001) Blocking sp1 transcription factor broadly inhibits extracellular matrix gene expression in vitro and in vivo: implications for the treatment of tissue fibrosis *J Invest Dermatol* **116**, 755-763

Conflict of interest: No conflict of interest.
Author contributions: AD designed, performed and analysed all experiments in this study, conceived and coordinated the study and wrote the paper. KB contributed surgical procedures in rats, imaging procedures (Fig3) and writing of the manuscript. JT contributed Fig1A. BR performed LC-MS/MS procedures and wrote the LC-MS/MS methodology. EJB supervised the study and contributed to experimental design and writing of the manuscript.
All authors reviewed results and approved the submitted manuscript.

FIGURE LEGENDS

Figure 1: Comparing rat and axolotl spinal cord injury microarrays to identify common differentially regulated genes. A: The 4-direction scatter-plot depicts shared differentially regulated genes identified in rat and axolotl microarrays 7 days post-SCI. Only transcripts with adjusted *p* value ≤0.05 and fold-change ≥2 (see **Supplemental Tables 1** & **2**) were included. Shared differentially regulated transcripts were split into 4 groups according to their log fold-change in rat and axolotl microarrays: *Group 1* genes were upregulated in axolotls but downregulated in rats; *Group 2* genes were upregulated in both species; *Group 3* genes were downregulated in both species and *Group 4* genes were upregulated in rats but downregulated in axolotls. Highly differentially regulated genes across species are indicated (red and text) and significant biological process GO terms found using BinGO are shown. **B**: The graph summarises the number of shared genes from intersection of rat and axolotl microarrays 7 days post-SCI and their group distribution. **C**: Protein-Protein interaction network depicting the shared cluster of genes with GO terms "ECM organization" and "vasculature development" from *Group 2*. These genes are upregulated in both rats and axolotls 7 days after SCI. Network was made using StringDB and Cytoscape.

Figure 2: High-throughput proteomics validates the differential regulation of multiple transcripts at the protein level following rat SCI. A-B: Heat-maps summarize significantly altered (T-Test $p \geq 0.05$) proteins identified by shot-gun proteomics and quantified by spectral counting, 7 days after rat SCI (**Supplemental Tables 3** & **4**). These proteins had matching upregulated and downregulated transcripts in the rat microarray and were either upregulated (**A**) or downregulated (**B**) in the axolotl microarray. **C-D**: Protein-protein interaction networks of axolotl upregulated (**C**) or downregulated (**D**) intersecting proteins. **E**: Multiple proteins from **A** & **C** were validated using immunoblotting in intact or injured T10 rat spinal cord extracts 7 days post-SCI.

Figure 3: Collagen-1 signature and aberrant vascular remodelling after rat SCI. A-E: Immunofluorescence staining of collagen-1 (red; antibody recognises both COL1A1 and COL1A2 chains) and CD34 (green) in either T10 injury epicentre sections (**A**) 2 weeks post-SCI or intact control T10 spinal cord (**D**). (**B**) is a magnified area from (**A**) and (**C**) is an image taken with a 60x oil objective. (**E**) is a magnified area from (**D**). **F-I**: Immunofluorescence staining of PDGFRα (red) and CD34 (green) in either T10 injury epicentre sections (**F**) or intact T10 spinal cord (**J**). (**G**) is a magnified area from (**F**) and (**H**) is a 60x oil objective image from (**F**). (**I**) is a magnified area from (**J**). Results are representative of at least 4 different immunostained spinal cords. **K**: TagMan qPCR of intact and injured spinal cord segments 2 weeks post-SCI. ** $p \geq 0.01$, *** $p \geq 0.001$ T-Test; 6 intact vs 6 injured spinal cords. Data is mean +SD. **L**: 10 Transcription factors with most predicted DNA binding sites for genes shown in **Fig. 2A-B**. Number of likely target genes is shown in the *x axis*. **M-N**: Immunoblotting and densitometry of selected proteins potentially regulated by SP1 in injured T10 spinal cord tissue extracts. Rats were IP injected daily with either vehicle solution (Veh; 10% DMSO in saline) or 0.2mg/kg mithramycin A (+Mith). Animals were sacrificed 2 weeks post-SCI. * $p \geq 0.05$, ** $p \geq 0.01$, *** $p \geq 0.001$ T-Test; 3 vehicle treated vs 3 mithramycin A treated SCI rats. Data is mean +SD.

Figure 1

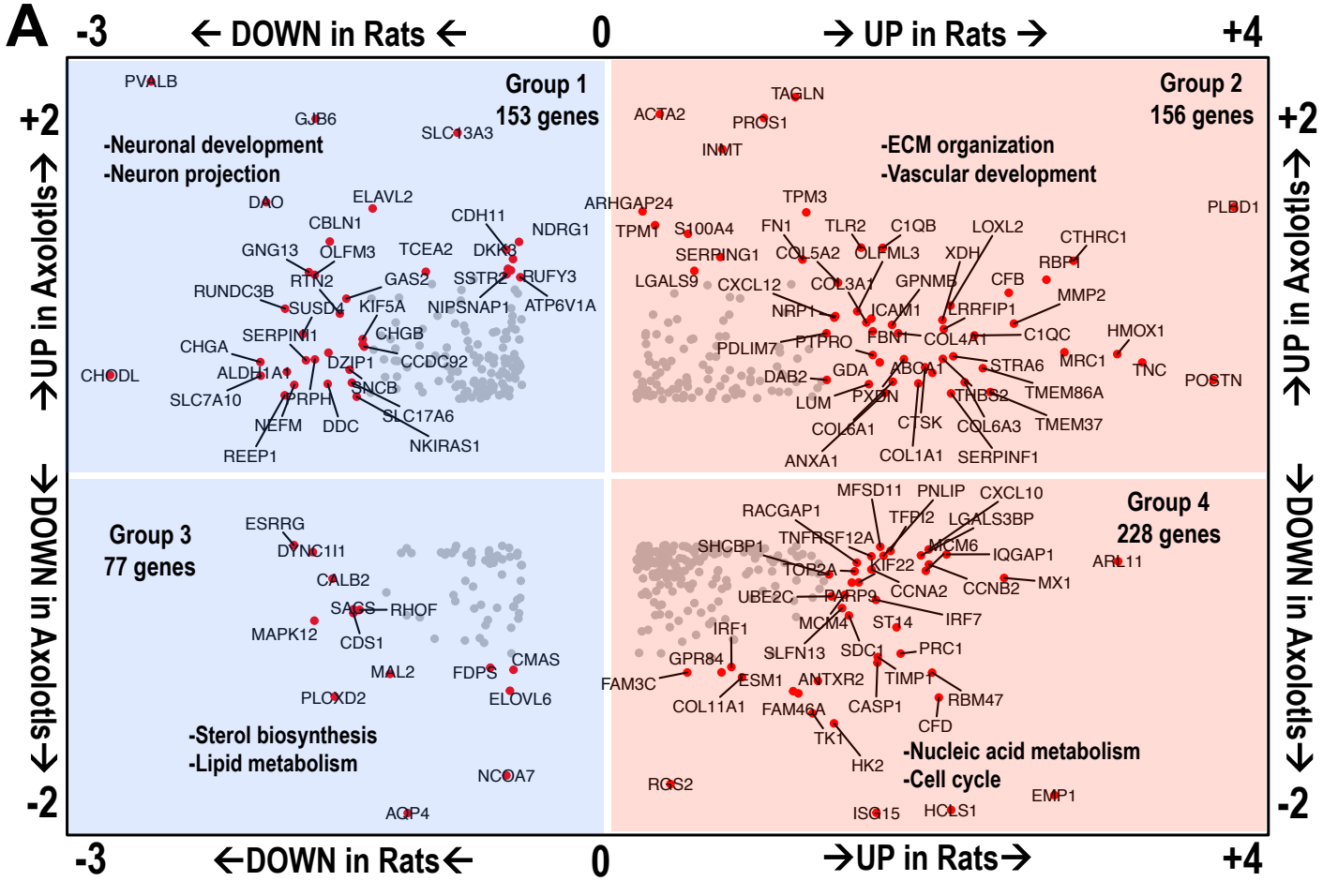
A
-3
← DOWN in Rats ←
0
→ UP in Rats →
+4
+2
→UP in Axolotls→
-2
←DOWN in Axolotls←
Group 1
153 genes
-Neuronal development
-Neuron projection
PVALB
GJB6
SLC13A3
DAO
ELAVL2
CBLN1
CDH11
NDRG1
GNG13
OLFM3
TCEA2
DKK3
RTN2
GAS2
SSTR2
RUFY3
RUNDC3B
SUSD4
KIF5A
NIPSNAP1
ATP6V1A
SERPINI1
CHGB
CHGA
DZIP1
CCDC92
CHODL
ALDH1A1
SNCB
SLC7A10
PRPH
SLC17A6
NEFM
DDC
NKIRAS1
REEP1
Group 2
156 genes
-ECM organization
-Vascular development
TAGLN
ACTA2
PROS1
INMT
ARHGAP24
TPM3
PLBD1
TPM1
S100A4
FN1
TLR2
C1QB
LOXL2
CTHRC1
SERPING1
COL5A2
OLFML3
XDH
RBP1
LGALS9
CXCL12
COL3A1
GPNMB
CFB
MMP2
NRP1
ICAM1
LRRFIP1
C1QC
HMOX1
PDLIM7
PTPRO
FBN1
COL4A1
MRC1
TNC
POSTN
DAB2
GDA
ABCA1
STRA6
LUM
PXDN
THBS2
TMEM86A
COL6A1
CTSK
COL6A3
TMEM37
ANXA1
COL1A1
SERPINF1
Group 3
77 genes
ESRRG
DYNC1I1
CALB2
SAGS
RHOF
MAPK12
CDS1
CMAS
MAL2
FDPS
PLOXD2
ELOVL6
-Sterol biosynthesis
-Lipid metabolism
NCOA7
AQP4
Group 4
228 genes
-Nucleic acid metabolism
-Cell cycle
MFSD11
PNLIP
CXCL10
RACGAP1
TFPI2
LGALS3BP
TNFRSF12A
SHCBP1
MCM6
IQGAP1
ARL11
TOP2A
KIF22
MX1
CCNA2
CCNB2
UBE2C
PARP9
IRF7
IRF1
MCM4
ST14
GPR84
SLFN13
SDC1
PRC1
FAM3C
ESM1
ANTXR2
TIMP1
RBM47
COL11A1
FAM46A
CASP1
CFD
TK1
HK2
RGS2
EMP1
ISG15
HCLS1

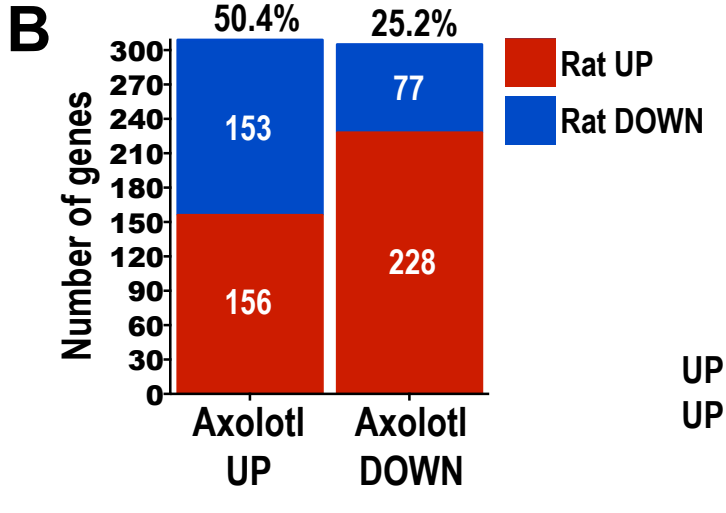
B
50.4%
25.2%
Number of genes
300
270
240
210
180
150
120
90
60
30
0
153
156
77
228
Rat UP
Rat DOWN
Axolotl UP
Axolotl DOWN

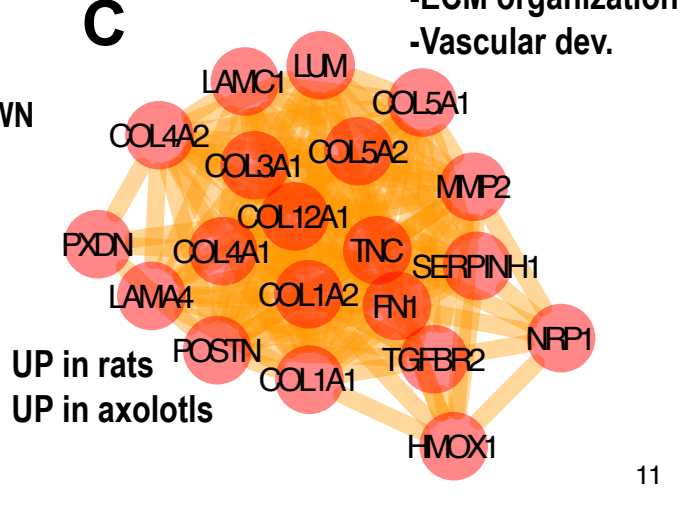
C
-ECM organization
-Vascular dev.
LAMC1
LUM
COL5A1
COL4A2
COL3A1
COL5A2
MMP2
COL12A1
PXDN
COL4A1
TNC
SERPINH1
LAMA4
COL1A2
FN1
NRP1
POSTN
TGFBR2
COL1A1
HMOX1
UP in rats
UP in axolotls

Figure 2

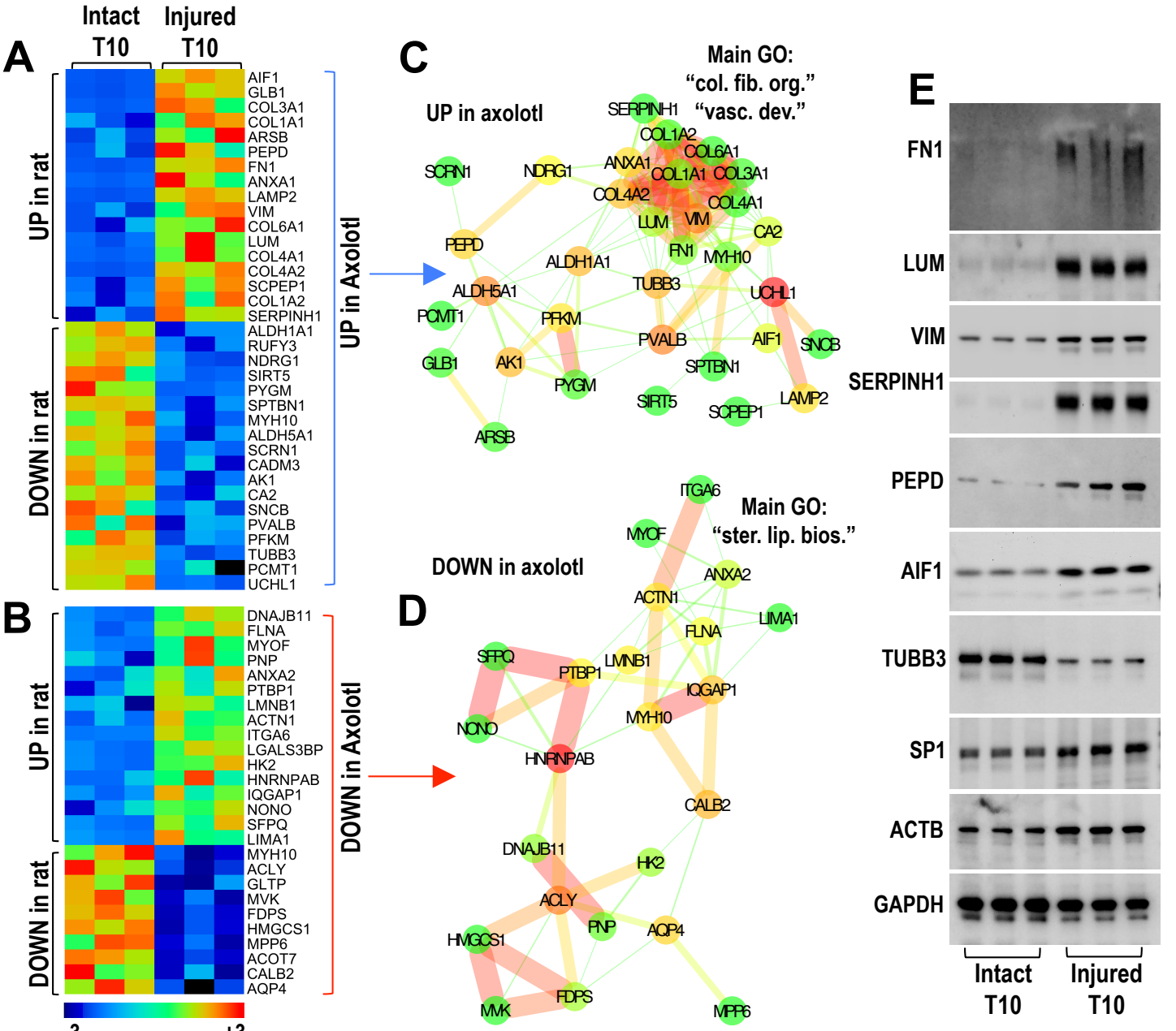
A
Intact T10
Injured T10
UP in rat
DOWN in rat
UP in Axolotl
AIF1
GLB1
COL3A1
COL1A1
ARSB
PEPD
FN1
ANXA1
LAMP2
VIM
COL6A1
LUM
COL4A1
COL4A2
SCPEP1
COL1A2
SERPINH1
ALDH1A1
RUFY3
NDRG1
SIRT5
PYGM
SPTBN1
MYH10
ALDH5A1
SCRN1
CADM3
AK1
CA2
SNCB
PVALB
PFKM
TUBB3
PCMT1
UCHL1
B
UP in rat
DOWN in rat
DOWN in Axolotl
DNAJB11
FLNA
MYOF
PNP
ANXA2
PTBP1
LMNB1
ACTN1
ITGA6
LGALS3BP
HK2
HNRNPAB
IQGAP1
NONO
SFPQ
LIMA1
MYH10
ACLY
GLTP
MVK
FDPS
HMGCS1
MPP6
ACOT7
CALB2
AQP4
-3
+3
C
UP in axolotl
Main GO:
"col. fib. org."
"vasc. dev."
SERPINH1
COL1A2
COL6A1
ANXA1
COL1A1
COL3A1
SCRN1
NDRG1
COL4A2
COL4A1
LUM
VIM
CA2
PEPD
FN1
MYH10
ALDH1A1
TUBB3
ALDH5A1
UCHL1
PCMT1
PFKM
PVALB
AIF1
SNCB
GLB1
AK1
SPTBN1
PYGM
SIRT5
LAMP2
SCPEP1
ARSB
D
DOWN in axolotl
Main GO:
"ster. lip. bios."
ITGA6
MYOF
ANXA2
ACTN1
LIMA1
FLNA
SFPQ
LMNB1
PTBP1
IQGAP1
MYH10
NONO
HNRNPAB
CALB2
DNAJB11
HK2
ACLY
PNP
AQP4
HMGCS1
FDPS
MVK
MPP6
E
FN1
LUM
VIM
SERPINH1
PEPD
AIF1
TUBB3
SP1
ACTB
GAPDH
Intact T10
Injured T10

Figure 3

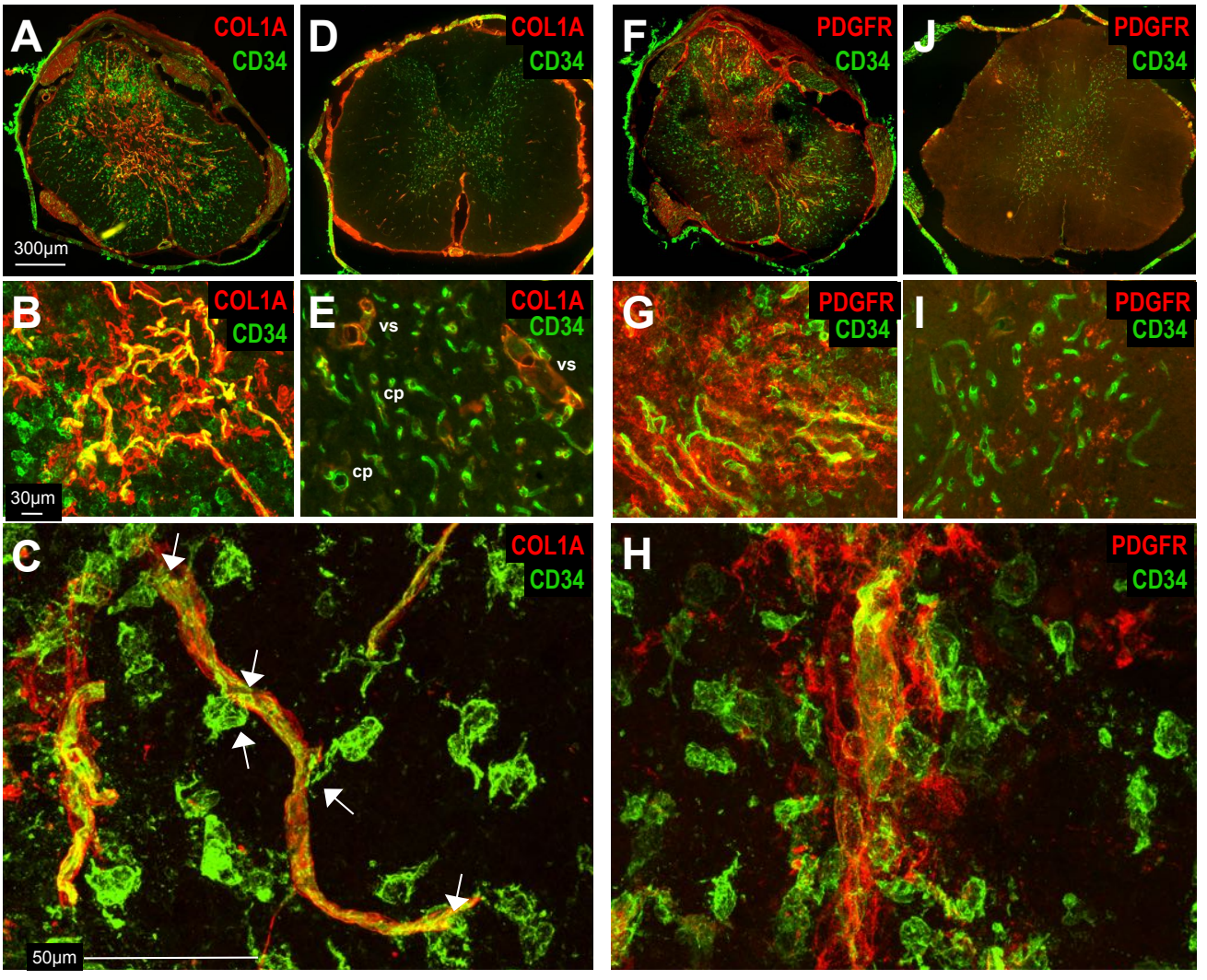
A
COL1A
CD34
300µm
D
COL1A
CD34
F
PDGFR
CD34
J
PDGFR
CD34
B
COL1A
CD34
30µm
E
COL1A
CD34
vs
cp
cp
vs
G
PDGFR
CD34
I
PDGFR
CD34
C
COL1A
CD34
50µm
H
PDGFR
CD34

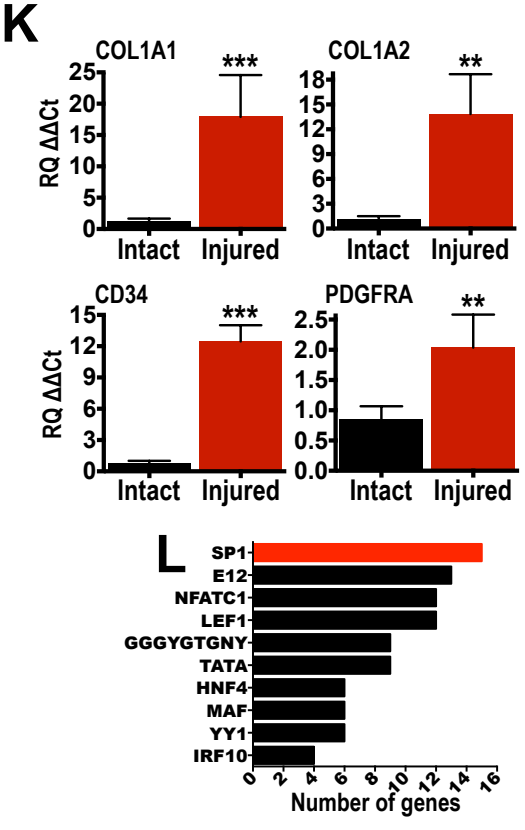
K
COL1A1
COL1A2
CD34
PDGFRA
RQ ΔΔCt
Intact
Injured
***
**
L
SP1
E12
NFATC1
LEF1
GGGYGTGNY
TATA
HNF4
MAF
YY1
IRF10
Number of genes

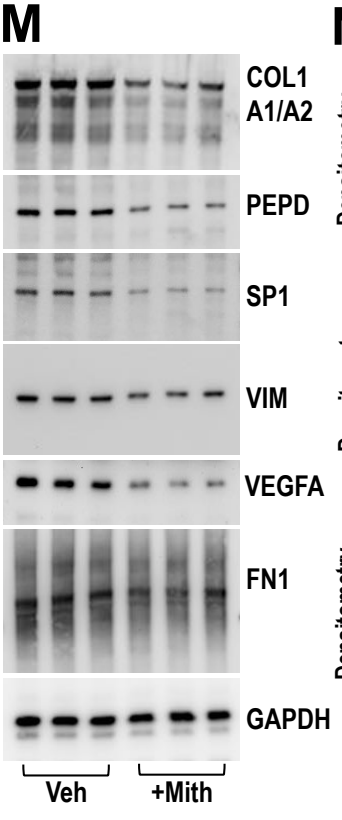
M
COL1
A1/A2
PEPD
SP1
VIM
VEGFA
FN1
GAPDH
Veh
+Mith

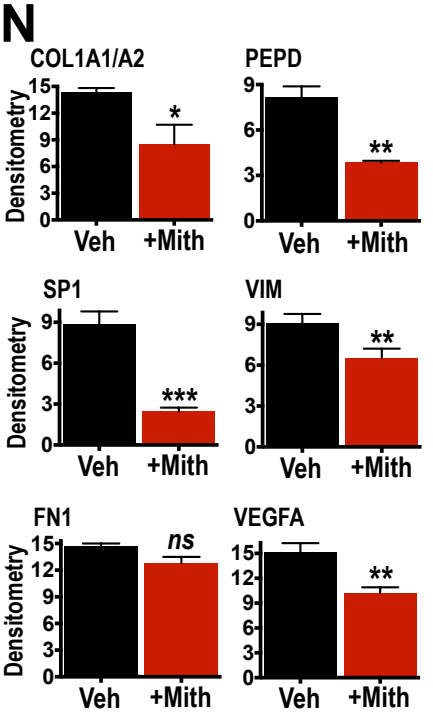
N
COL1A1/A2
PEPD
SP1
VIM
FN1
VEGFA
Densitometry
Veh
+Mith
*
**
***
ns